Excitation and Detection Efficiency Under Light-Sheet Illumination

Talon Chandler

June 21, 2017
(Updated: June 26, 2017)

1 Introduction

In these notes I will calculate the excitation and detection efficiency of a single fluorophore under polarized scanned light-sheet illumination. I will start by finding the transverse and longitudinal fields at all positions in a Gaussian beam using reasonable approximations. Next I will calculate the excitation efficiency of a single fluorophore as the beam is scanned across the fluorophore. I will combine these results with the results from previous notes to write the complete forward model. Finally I will discuss the approximations we may need to simplify reconstruction.

2 Transverse and Longitudinal Fields In A Scanned Gaussian Beam

The complex spatial electric field of a paraxial Gaussian beam propagating along the $\hat{\mathbf{z}}$ axis is [1]

$$\mathbf{E}(x,y,z) = \mathbf{A}\frac{w_0}{w(z)}\exp\left\{-\frac{(x^2+y^2)}{w^2(z)} + i\left[kz - \eta(z) + \frac{k(x^2+y^2)}{2R(z)}\right]\right\} \tag{1}$$

where

$$\mathbf{A} = \cos\phi_{\text{pol}}\hat{\mathbf{x}} + \sin\phi_{\text{pol}}\hat{\mathbf{y}} \qquad \text{is the input Jones vector in 3D,} \tag{2}$$

$$w_0 \approx \frac{2n}{k(\text{NA})} \qquad \text{is the beam waist radius,} \tag{3}$$

$$z_0 = \frac{kw_0^2}{2} \qquad \text{is the Rayleigh range,} \tag{4}$$

$$k = \frac{2\pi n}{\lambda} \qquad \text{is the wave number,} \tag{5}$$

$$w(z) = w_0\sqrt{1+\frac{z^2}{z_0^2}} \qquad \text{is the beam radius,} \tag{6}$$

$$R(z) = z\left(1+\frac{z_0^2}{z^2}\right) \qquad \text{is the wavefront radius,} \tag{7}$$

$$\eta(z) = \arctan\left(\frac{z}{z_0}\right) \qquad \text{is the phase correction.} \tag{8}$$

Equation 1 uses the paraxial approximation, so it can only be used for beams with a waist that is significantly larger than the reduced wavelength ($w_0 \gg \lambda/n$). Notice that under the paraxial approximation the beam is uniformly polarized in the transverse plane.

We would like to calculate the longitudinal component of a Gaussian beam when the beam waist approaches the reduced wavelength ($w_0 > \lambda/n$). One approach is to numerically evaluate the Richards-Wolf diffraction integral [2, 3]. This approach is time consuming and too accurate for our needs—we only want to model weak longitudinal fields. Instead, I will follow Novotny et. al. [1] and use a longitudinal correction to equation 1.

As written, equation 1 doesn't satisfy Gauss' law ($\nabla \cdot \mathbf{E} = 0$), so we will add a longitudinal field to correct it. If the input beam is polarized along the $\hat{\mathbf{x}}$ axis ($\phi_{\text{pol}} = 0$), then we can rearrange Gauss' law to relate the

longitudinal and transverse fields with

$$E_z(x,y,z) = -\int \left[\frac{\partial}{\partial x} E_x(x,y,z)\right] dz. \tag{9}$$

Carnicer et al. [4] worked through this integral using the angular spectrum representation and found that

$$E_z(x,y,z) = -i\frac{2x}{kw_0^2} E_x(x,y,z) = -i\frac{x}{z_0} E_x(x,y,z). \tag{10}$$

Equation 10 means that:

- There is no longitudinal polarization in the $\hat{\mathbf{y}} - \hat{\mathbf{z}}$ plane because $E_z(0,y,z) = 0$.
- There are longitudinal field lobes on both sides of the optical axis along the transverse polarization direction.
- The factor of i means that the longitudinal fields are 90° out of phase with the transverse fields which means that the total field is elliptically polarized off axis.
- The longitudinal field strength is proportional to λ/w_0^2—highly focused beams have the strongest longitudinal fields.

If the input is polarized along the $\hat{\mathbf{x}}$ axis, the corrected 3D Jones vector is

$$\mathbf{A}(x,y,z) = \hat{\mathbf{x}} - i\frac{x}{z_0}\hat{\mathbf{z}}. \tag{11}$$

If the input polarization is arbitrary then the corrected 3D Jones vector is

$$\mathbf{A}(x,y,z) = \cos\phi_{\text{pol}}\hat{\mathbf{x}} + \sin\phi_{\text{pol}}\hat{\mathbf{y}} - i\frac{x\cos\phi_{\text{pol}} + y\sin\phi_{\text{pol}}}{z_0}\hat{\mathbf{z}}. \tag{12}$$

If the beam is scanned along the $\hat{\mathbf{y}}$ axis with velocity v then the time dependent 3D Jones vector is

$$\mathbf{A}(x,y,z,t) = \cos\phi_{\text{pol}}\hat{\mathbf{x}} + \sin\phi_{\text{pol}}\hat{\mathbf{y}} - i\frac{x\cos\phi_{\text{pol}} + (y-vt)\sin\phi_{\text{pol}}}{z_0}\hat{\mathbf{z}} \tag{13}$$

and the time-dependent electric field is

$$\mathbf{E}(x,y,z,t) = \mathbf{A}(x,y,z,t)\frac{w_0}{w(z)}\exp\left\{-\frac{(x^2+(y-vt)^2)}{w^2(z)} + i\left[kz - \eta(z) + \frac{k(x^2+(y-vt)^2)}{2R(z)}\right]\right\}. \tag{14}$$

We will use equations 13 and 14 to calculate the excitation efficiency of a single fluorophore. Notice that as the Rayleigh range z_0 increases the longitudinal electric field decreases, so we can ignore the longitudinal component when the beam is weakly focused.

3 Scanned Beam Excitation Efficiency

We define the excitation efficiency of a fluorophore as the fraction of incident power that excites the fluorophore. If a fluorophore with absorption dipole moment $\boldsymbol{\mu}_{\text{abs}}$ is placed in a time-independent complex electric field $\mathbf{E}$, then the excitation efficiency is given by

$$\eta_{\text{exc}} = \frac{|\boldsymbol{\mu}_{\text{abs}} \cdot \mathbf{E}(x,y,z)|^2}{|\mathbf{E}(x,y,z)|^2}. \tag{15}$$

If the fluorophore is placed in the path of a scanned laser then the electric field becomes time dependent. If the laser is scanned quickly we would need to consider the coherence of the electric field, but we will only consider slow scanning here to simplify the calculation. Specifically, we require that $v \ll w_0/\tau_c$—the scan velocity must be much less than the beam width divided by the coherence time. In this case the excitation efficiency is

$$\eta_{\text{exc}} = \frac{\int_{-\infty}^{\infty} |\boldsymbol{\mu}_{\text{abs}} \cdot \mathbf{E}(x,y,z,t)|^2 dt}{\int_{-\infty}^{\infty} |\mathbf{E}(x,y,z,t)|^2 dt} \tag{16}$$

We plug equation 14 into equation 16, express $\boldsymbol{\mu}_{\text{abs}}$ in spherical coordinates

$$\boldsymbol{\mu}_{\text{abs}} = \cos\Phi \sin\Theta \hat{\mathbf{x}} + \sin\Phi \sin\Theta \hat{\mathbf{y}} + \cos\Theta \hat{\mathbf{z}}, \tag{17}$$

and evaluate the integrals (see Appendix for details) to write the excitation efficiency as

$$\eta_{\text{exc}} = \frac{\sin^2\Theta \cos^2(\Phi - \phi_{\text{pol}}) + \cos^2\Theta \frac{x^2 \cos^2\phi_{\text{pol}} + \frac{1}{4}w^2(z)\sin^2\phi_{\text{pol}}}{z_0^2}}{1 + \frac{x^2 \cos^2\phi_{\text{pol}} + \frac{1}{4}w^2(z)\sin^2\phi_{\text{pol}}}{z_0^2}}. \tag{18}$$

If the beam is weakly focused then we can ignore the longitudinal excitation and the excitation efficiency simplifies to

$$\eta_{\text{exc}} \approx \sin^2\Theta \cos^2(\Phi - \phi_{\text{pol}}). \tag{19}$$

How good is the approximation in equation 19?

For longitudinal fluorophores equation 19 is a very bad approximation—it predicts that a longitudinal fluorophore will not be excited at all. We can't use a percentage error because the approximation completely ignores the excitation of longitudinal dipoles.

Instead, we can compare the size of signals from longitudinal and transverse fluorophores. If the signal from longitudinal fluorophores is less than the signal from noise and background, then we can ignore the signal from longitudinal fluorophores.

$$\text{Excitation Ratio} = \frac{\text{Max Longitudinal Excitation}}{\text{Max Transverse Excitation}} \tag{20}$$

$$= \frac{\eta_{\text{exc}}(\Theta = 0)}{\eta_{\text{exc}}(\Theta = \pi/2, \Phi = \phi_{\text{pol}})} \tag{21}$$

$$= \frac{x^2 \cos^2\phi_{\text{pol}} + \frac{1}{4}w^2(z)\sin^2\phi_{\text{pol}}}{z_0^2} \tag{22}$$

At first glance equation 22 looks bleak—the excitation ratio grows without bound in the x direction which means that the longitudinal excitation becomes a larger fraction of the total excitation as we move away from the plane of the light-sheet. Fortunately, we only care about regions of the beam with a high intensity, so we look at the intensity-weighted excitation ratio instead.

$$\text{Intensity-Weighted Excitation Ratio} = \frac{w_0}{w(z)} e^{-\frac{2x^2}{w^2(z)}} \frac{x^2 \cos^2\phi_{\text{pol}} + \frac{1}{4}w^2(z)\sin^2\phi_{\text{pol}}}{z_0^2}$$

We can interpret the intensity-weighted excitation ratio as the fraction of the maximum signal (created by a transverse fluorophore at the origin) that we ignore by ignoring longitudinal excitation. Figure 1 shows that the intensity weighted excitation ratio is <2% for the imaging parameters used in Wu et. al. [5].

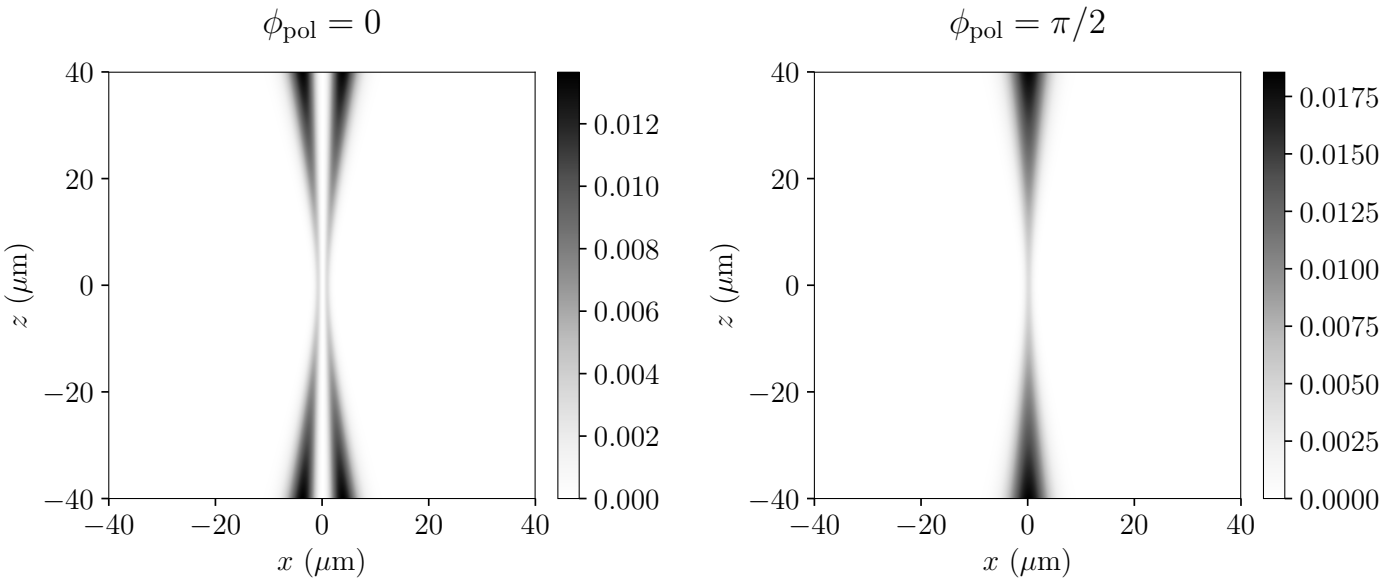

Figure 1: Intensity-weighted excitation ratio as a function of position using the parameters in Wu et. al. [5]: $w_0 = 1.2$ μm, $z_0 = 9$ μm, $\lambda = 488$ nm, FOV$\approx$ 80×80 μm^2. The maximum values are at the edge of the FOV and are <2%.

As a rough heuristic, if the fraction of the signal from noise and background is greater than the intensity-weighted excitation ratio we can justifiably ignore the longitudinal component.

Figure 2 shows the maximum intensity-weighted excitation ratio for an 80×80 μm^2 FOV as a function of w_0. The maximum intensity-weighted excitation ratio decreases as w_0 increases because wider beams have smaller longitudinal components.

4 Detection Efficiency

If we detect fluorescence in wide-field mode with an orthogonal arm and no polarizer then the detection efficiency is

$$\eta_{\text{det}} = 2A + 2B \sin^2 \Theta' \tag{23}$$

where

$$A = \frac{1}{4} - \frac{3}{8}\cos\alpha + \frac{1}{8}\cos^3\alpha, \tag{24}$$

$$B = \frac{3}{16}\cos\alpha - \frac{3}{16}\cos^3\alpha, \tag{25}$$

$\alpha = \arcsin(\text{NA}/n)$ is the detection cone half angle, and Θ' is the angle between the dipole axis and the detection optical axis. See the 2017-06-09 notes for the relationship between Θ' and Θ, Φ. See [6] and the 2017-04-25 notes for the derivation of the detection efficiencies and additional expression for detection arms that use a polarizer.

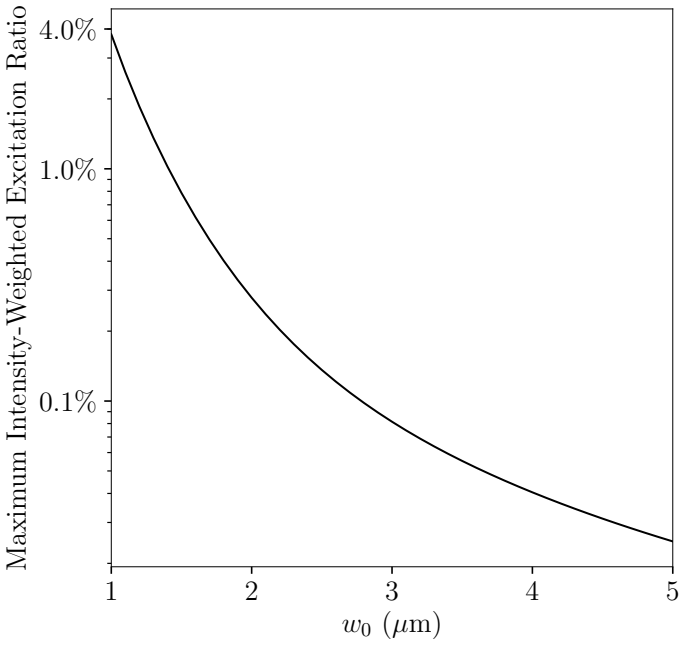

Figure 2: Maximum intensity-weighted excitation ration (see equation 23) for an 80×80 μm^2 FOV with $\lambda = 488$ nm.

5 Orientation Forward Model

The detected intensity is proportional to the the product of the excitation and detection efficiencies. Using a weakly focused excitation beam and an unpolarized detection arm gives us the following model

$$I_{\phi_{\text{pol}}} = I_{\text{tot}} \sin^2\Theta \cos^2(\Phi - \phi_{\text{pol}})(2A + 2B\sin^2\Theta') \tag{26}$$

where I_{tot} is the intensity we would collect if we had an excitation and detection efficiency of 1.

6 Discussion

Equation 18 shows that for strongly focused beams the excitation efficiency is a function of position. This couples the orientation and location of the fluorophore and complicates our reconstruction. For now we'll use only weakly focused beams so that we can ignore the longitudinal component.

To ignore the longitudinal component, we require that the fraction of the signal from noise and background is greater than the intensity weighted excitation ratio ($<$2% with current imaging parameters). We'll need to be careful about longitudinal excitation if we want to use beams that are more strongly focused.

Under the weak-focusing approximation the orientation and position of fluorophores are decoupled. This will allow us to split the reconstruction into two steps (1) estimate the position of the fluorophores using unpolarized frames (or the sum of orthogonally polarized frames) with established reconstruction techniques then (2) estimate the orientation or the fluorophores using polarized frames and equation 26.

Note that we are working in a different regime than Agrawal et. al. [7]. They are considering imaging systems with better resolution than ours, so the position and orientation are coupled and must be estimated together. At our resolution, the position and orientation are decoupled so we can estimate them separately.

7 References

[1] Lukas Novotny and Bert Hecht. *Principles of Nano-Optics*. English. Cambridge University Press, 2006. URL: https://www.photonics.ethz.ch/fileadmin/user_upload/Courses/NanoOptics/.

[2] B. Richards and E. Wolf. "Electromagnetic Diffraction in Optical Systems. II. Structure of the Image Field in an Aplanatic System." In: *Proceedings of the Royal Society of London A: Mathematical, Physical and Engineering Sciences* 253.1274 (1959), pp. 358–379. URL: http://rspa.royalsocietypublishing.org/content/253/1274/358.

[3] Martin Weigert, Eugene W. Myers, and Moritz Kreysing. "Biobeam - Rigorous wave-optical simulations of light-sheet microscopy." In: (2017). URL: https://arxiv.org/abs/1706.02261.

[4] Artur Carnicer et al. "On the longitudinal component of paraxial fields." In: *European Journal of Physics* 33.5 (2012), p. 1235. URL: http://stacks.iop.org/0143-0807/33/i=5/a=1235.

[5] Yicong Wu et al. "Spatially isotropic four-dimensional imaging with dual-view plane illumination microscopy." In: *Nat Biotech* 31.11 (Nov. 2013). Research, pp. 1032–1038. ISSN: 1087-0156. URL: http://www.nature.com/nbt/journal/v31/n11/full/nbt.2713.html.

[6] John T. Fourkas. "Rapid determination of the three-dimensional orientation of single molecules." In: *Opt. Lett.* 26.4 (Feb. 2001), pp. 211–213. URL: http://ol.osa.org/abstract.cfm?URI=ol-26-4-211.

[7] Anurag Agrawal et al. "Limits of 3D dipole localization and orientation estimation for single-molecule imaging: towards Green's tensor engineering." In: *Opt. Express* 20.24 (Nov. 2012), pp. 26667–26680. URL: http://www.opticsexpress.org/abstract.cfm?URI=oe-20-24-26667.

8 Appendix

We will evaluate the following integrals to find the excitation efficiency

$$\eta_{\text{exc}}(x,y,z) = \frac{\int_{-\infty}^{\infty} |\boldsymbol{\mu}_{\text{abs}} \cdot \mathbf{E}(x,y,z,t)|^2 dt}{\int_{-\infty}^{\infty} |\mathbf{E}(x,y,z,t)|^2 dt} \tag{27}$$

where

$$\boldsymbol{\mu}_{\text{abs}} = \cos\Phi \sin\Theta \hat{\mathbf{x}} + \sin\Phi \sin\Theta \hat{\mathbf{y}} + \cos\Theta \hat{\mathbf{z}} \tag{28}$$

$$\mathbf{E}(x,y,z,t) = \mathbf{A}(x,y,z,t) \frac{w_0}{w(z)} \exp\left\{ -\frac{(x^2 + (y-vt)^2)}{w^2(z)} + i\left[kz - \eta(z) + \frac{k(x^2+(y-vt)^2)}{2R(z)} \right] \right\} \tag{29}$$

$$\mathbf{A}(x,y,z,t) = \cos\phi_{\text{pol}} \hat{\mathbf{x}} + \sin\phi_{\text{pol}} \hat{\mathbf{y}} - i \frac{x\cos\phi_{\text{pol}} + (y-vt)\sin\phi_{\text{pol}}}{z_0} \hat{\mathbf{z}}. \tag{30}$$

We'll need the following facts

$$\int_{-\infty}^{\infty} e^{-ax^2} dx = \sqrt{\frac{\pi}{a}} \tag{31}$$

$$\int_{-\infty}^{\infty} x e^{-ax^2} dx = 0 \tag{32}$$

$$\int_{-\infty}^{\infty} x^2 e^{-ax^2} dx = \frac{1}{2a}\sqrt{\frac{\pi}{a}}. \tag{33}$$

The numerator is

$$= \int_{-\infty}^{\infty} |\boldsymbol{\mu}_{\text{abs}} \cdot \mathbf{E}(x,y,z,t)|^2 dt \tag{34}$$

$$\begin{aligned} = \int_{-\infty}^{\infty} \Bigg| &\left[\cos\Phi \sin\Theta \cos\phi_{\text{pol}} + \sin\Phi \sin\Theta \sin\phi_{\text{pol}} - i\cos\Theta \frac{x\cos\phi_{\text{pol}} + (y-vt)\sin\phi_{\text{pol}}}{z_0} \right] \\ &\frac{w_0}{w(z)} \exp\left\{ -\frac{(x^2+(y-vt)^2)}{w^2(z)} + i\left[kz - \eta(z) + \frac{k(x^2+(y-vt)^2)}{2R(z)} \right] \right\} \Bigg|^2 dt. \end{aligned} \tag{35}$$

After changing variables $y' = y - vt$ and moving constants outside the integral we get

$$= \frac{w_0^2}{w^2(z)} e^{-\frac{2x^2}{w^2(z)}} \int_{-\infty}^{\infty} \left| \left[\cos\Phi \sin\Theta \cos\phi_{\text{pol}} + \sin\Phi \sin\Theta \sin\phi_{\text{pol}} - i\cos\Theta \frac{x\cos\phi_{\text{pol}} + y'\sin\phi_{\text{pol}}}{z_0} \right] \right|^2 e^{-\frac{2y'^2}{w^2(z)}} dy'. \tag{36}$$

After expanding the square brackets we get

$$= \frac{w_0^2}{w^2(z)} e^{-\frac{2x^2}{w^2(z)}} \int_{-\infty}^{\infty} \left[(\cos\Phi \sin\Theta \cos\phi_{\text{pol}} + \sin\Phi \sin\Theta \sin\phi_{\text{pol}})^2 + \cos^2\Theta \frac{(x\cos\phi_{\text{pol}} + y'\sin\phi_{\text{pol}})^2}{z_0^2} \right] e^{-\frac{2y'^2}{w^2(z)}} dy' \tag{37}$$

$$= \frac{w_0^2}{w(z)} e^{-\frac{2x^2}{w^2(z)}} \sqrt{\frac{\pi}{2}} \left[\sin^2\Theta \cos^2(\Phi - \phi_{\text{pol}}) + \cos^2\Theta \frac{x^2\cos^2\phi_{\text{pol}} + \frac{1}{4}w^2(z)\sin^2\phi_{\text{pol}}}{z_0^2} \right]. \tag{38}$$

The denominator is

$$= \int_{-\infty}^{\infty} |\mathbf{E}(x,y,z,t)|^2 dt \tag{39}$$

$$= \frac{w_0^2}{w^2(z)} e^{-\frac{2x^2}{w^2(z)}} \int_{-\infty}^{\infty} \left| \left[\cos\phi_{\text{pol}} \hat{\mathbf{x}} + \sin\phi_{\text{pol}} \hat{\mathbf{y}} - i \frac{x\cos\phi_{\text{pol}} + y' \sin\phi_{\text{pol}}}{z_0} \hat{\mathbf{z}} \right] \right|^2 e^{-\frac{2y'^2}{w^2(z)}} dy' \tag{40}$$

$$= \frac{w_0^2}{w^2(z)} e^{-\frac{2x^2}{w^2(z)}} \int_{-\infty}^{\infty} \left[1 + \frac{(x\cos\phi_{\text{pol}} + y' \sin\phi_{\text{pol}})^2}{z_0^2} \right] e^{-\frac{2y'^2}{w^2(z)}} dy' \tag{41}$$

$$= \frac{w_0^2}{w(z)} e^{-\frac{2x^2}{w^2(z)}} \sqrt{\frac{\pi}{2}} \left[1 + \frac{x^2\cos^2\phi_{\text{pol}} + \frac{1}{4} w^2(z) \sin^2\phi_{\text{pol}}}{z_0^2} \right]. \tag{42}$$

The final excitation efficiency is

$$\eta_{\text{exc}}(x,y,z) = \frac{\sin^2\Theta \cos^2(\Phi - \phi_{\text{pol}}) + \cos^2\Theta \frac{x^2\cos^2\phi_{\text{pol}} + \frac{1}{4} w^2(z)\sin^2\phi_{\text{pol}}}{z_0^2}}{1 + \frac{x^2\cos^2\phi_{\text{pol}} + \frac{1}{4} w^2(z)\sin^2\phi_{\text{pol}}}{z_0^2}}.$$